Supporting Information

Screening Versatile Water/Adsorbent Working Pairs for Wide Operation Conditions of Adsorption Heat Pumps

Zhilu Liu, [a] Wei Li, [b] Shanshan Cai,[a] Zhengkai Tu,[a] Xiaobing Luo,[a] Song Li [a,*]

[a] School of Energy and Power Engineering, Huazhong University of Science and Technology, Wuhan 430074, China.

[b] Energy & Electricity Research Center, Jinan University, Zhuhai 519070, China.

* Corresponding author email: songli@hust.edu.cn.

S1. Supplementary data in excel

Table S1. Literature for 231 adsorbents investigated in this work. (In the supplementary excel file)

Table S2. Fitting parameters of water adsorption isotherms using universal adsorption isotherm model. (In the supplementary excel file)

Table S3. Computational results of adsorption performance of adsorbent/water working pairs based on the maximum COP in adsorption cooling and heating system. (In the supplementary excel file)

Table S4. Computational results of adsorption performance of adsorbent/water working pairs based on the effective COP in adsorption cooling and heating system. (In the supplementary excel file)

S2. The experimental water adsorption isotherm database

The NIST/ARPA-E Database of Novel and Emerging Adsorbent Materials[1] contains a huge number of adsorption isotherms for various adsorbents and adsorbates collected from the literature. As of September 2018, 959 water adsorption isotherms were extracted from 329 publications in NIST database. After removing the simulated isotherms, as well as duplicated data, 288 experimental water adsorption isotherms with a temperature range of 288-308 K were obtained. We also excluded the isotherms with insufficient data points (i.e. < 10 points) for fitting and those measured at pressures higher than the saturation pressure of water at the relevant temperature. Finally, 231 experimental water adsorption isotherms (sources of them were shown in Table S1) were used for fitting by the universal adsorption isotherm model (UAIM)[2] applicable to various types of isotherms at different temperatures as described in Equation S1. The fitting parameters and fitting accuracy according to the chi-square goodness-of-fit test was shown in Table S2.

$$W = \sum_{i=1}^{n} \alpha_i \left\{ \frac{\left(\frac{p}{p_s} \exp\left(\frac{\varepsilon_i}{RT} \right) \right)^{\frac{RT}{m_i}}}{1 + \left(\frac{p}{p_s} \exp\left(\frac{\varepsilon_i}{RT} \right) \right)^{\frac{RT}{m_i}}} \right\}_i \quad \text{(Eq. S1)}$$

Where W is the equilibrium uptake, P and T represent the equilibrium pressure and temperature, P_0 is the saturation pressure of water and R is the ideal gas constant. α_i, ε_i, m_i and n are the four fitting parameters that are determined by the characteristic of the adsorption isotherms: α_i is the probability factor, where the sum of all of the probability factors is equal to 1, i.e. $\sum_{i=1}^{n} \alpha_i = 1$, ε_i and m_i depict the mean value and the standard deviation of the energy distribution curve, respectively.

The 231 adsorbents in the database can be classified into six categories as shown in Table S5, about 70% of which are MOFs followed by carbon, silicic materials, zeolites, composites and other materials.

Table S5. The number of different types of adsorbents.

Adsorbent species	Number
MOFs	163
Carbon	36
Zeolites	10
Silicic Materials	11
Composites [a]	7
Others [b]	4

[a] "Composites" include 6 carbon/another material composite and 1 polyoxometalate (POM)/MOF composite.

[b] "Others" include 2 metal oxides (MOs), 1 metal organophosphonate (MOP) and 1 POM.

S3. Computation details based on the basic thermodynamic cycle of AHP.

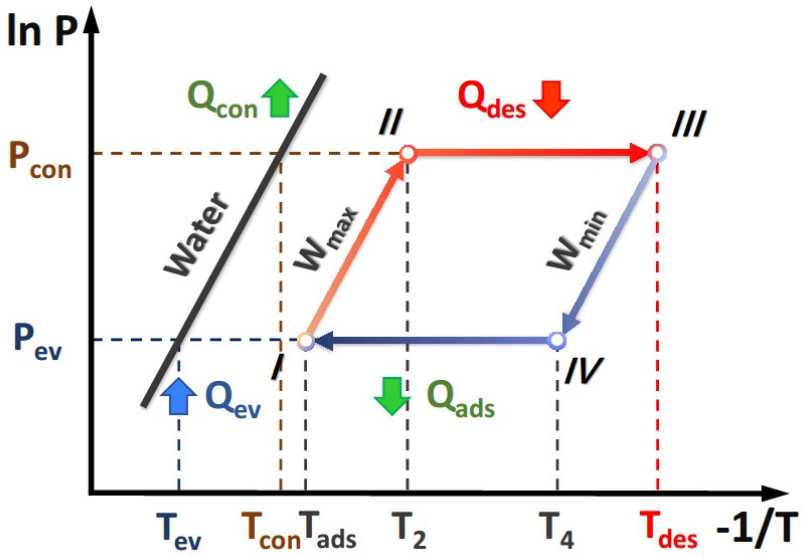

Figure S1. Basic thermodynamic cycle diagram of adsorption heat pump. The cycle is consisting of four steps: isosteric heating (I-II), isobaric desorption (II-III), isosteric cooling (III-IV) and isobaric adsorption (IV-I).

As shown in the basic thermodynamic cycle diagram of AHP (Figure S1), T_{ev} and T_{con} are the temperatures of evaporation and condensation, P_{ev} and P_{con} represent evaporation and condensation pressures, which equals the saturation pressure of water at T_{ev} and T_{con}, respectively. T_{ads} is adsorption temperature when adsorption process is completed, which equals T_{con} in this work. Similarly, T_{des} corresponds to the temperature at end of desorption process. T_2 (T_{des}^{min} in Table 1) and T_4 are starting temperatures of adsorption and desorption in the cycle, which can be obtained according to the generalized Trouton's rule[3] with fixed T_{ev}, T_{ads} and T_{des}, where $T_2 = T_{con}^2 / T_{ev}$ and $1/T_4 = 1/T_{des} - 1/T_2 + 1/T_{ads}$. Besides, the working capacity of water (ΔW) equals the difference of maximum water uptake (W_{max}) and minimum water uptake (W_{min}) (i.e. $\Delta W = W_{max} - W_{min}$), both

of them can be calculated by UAIM[2], these are $W_{max} = W(T_{ads}, P_{ev})$ and $W_{min} = W(T_{des}, P_{con})$.

Significantly, COP is defined as the energy taken up in the evaporator (SXE) divided by the energy required for regeneration of adsorbents (Q_{input}). COP_C for cooling and COP_H for heating can be defined by the following equations, respectively.

$$COP_C = \frac{SCE}{Q_{input}} = \frac{Q_{ev}}{Q_{des}} \quad \text{(Eq. S2)}$$

$$COP_H = \frac{SHE}{Q_{input}} = \frac{-(Q_{con} + Q_{ads})}{Q_{des}} \quad \text{(Eq. S3)}$$

Where, SCE is the specific cooling effects and SHE is the specific heating effects. SCE describes the energy transferred by working fluid for cooling, which equals the energy taken up in the evaporator (Q_{ev}), and Q_{input} is the heat energy from low-grade heat sources for desorption of adsorbent (Q_{des}). The useful energy output for heating is a combination of the energy released during condensation (Q_{con}) and the energy rejected during the adsorption stage (Q_{ads}), mindfully, both Q_{con} and Q_{ads} are negative values.

The calculation formulas of energy abovementioned are

$$Q_{ev} = \Delta W \Delta_{vap} H(T_{ev}) + \Delta W \int_{T_{con}}^{T_{ev}} C_p^{wf}(T) dT \quad \text{(Eq. S4)}$$

$$Q_{con} = \Delta W \left[-\Delta_{vap} H(T_{con}) \right] + \Delta W \int_{T_{ev}}^{T_{con}} C_p^{wf}(T) dT \quad \text{(Eq. S5)}$$

$$\begin{aligned} Q_{des} &= Q_{\text{I-II}} + Q_{\text{II-III}} \\ &= \left[\int_{T_{ads}}^{T_2} C_p^{ad}(T) dT + W_{max} \int_{T_{ads}}^{T_2} C_p^{wf}(T) dT \right] + \left[\int_{T_2}^{T_{des}} C_p^{ad}(T) dT + \int_{T_2}^{T_{des}} W(T) C_p^{wf}(T) dT + \int_{W_{max}}^{W_{min}} \Delta_{ads} H(W) dW \right] \end{aligned} \quad \text{(Eq. S6)}$$

$$\begin{aligned} Q_{ads} &= Q_{\text{III-IV}} + Q_{\text{IV-I}} \\ &= \left[\int_{T_{des}}^{T_4} C_p^{ad}(T) dT + W_{min} \int_{T_{des}}^{T_4} C_p^{wf}(T) dT \right] + \left[\int_{T_4}^{T_{ads}} C_p^{ad}(T) dT + \int_{T_4}^{T_{ads}} W(T) C_p^{wf}(T) dT + \int_{W_{min}}^{W_{max}} \Delta_{ads} H(W) dW \right] \end{aligned} \quad \text{(Eq. S7)}$$

Here, for the regeneration process of adsorbents (i.e. steps of I-II and II-III), $\int_{T_{ads}}^{T_2} C_p^{ad}(T)dT$ and $\int_{T_2}^{T_{des}} C_p^{ad}(T)dT$ are the energy required for the adsorbent bed temperature to change from T_{ads} to T_{des}, notably, we neglected the impact that not tunable of heat changer, only considered the effect of adsorbent. $W_{max}\int_{T_{ads}}^{T_2} C_p^{wf}(T)dT$ and $\int_{T_2}^{T_{des}} W(T)C_p^{ad}(T)dT$ are the energy required for the working fluid (water in this work) temperature from T_{ads} to T_{des},; the last term $\int_{W_{max}}^{W_{min}} \Delta_{ads}H(W)dW$ is the heat adsorbed for water desorption in the AHP system. A similar analysis was performed for the energy transfer during adsorption stage (Q_{ads}).

In these formulas, the specific heat capacity (C_p) of the adsorbent (C_p^{ad})and working fluid (C_p^{wf}) are considered to be constant (C_p varies slightly with temperature in fact), specifically, they are 1 (reasonable value for a variety of adsorbents)[4] and 4.2 kJ/(kg·K) (for water). Additionally, the vaporization enthalpy ($\Delta_{vap}H$, unit is kJ/kg) of water is a function of temperature.

$$\Delta_{vap}H(T) = -2.51(T-273)+2502 \quad \text{(Eq. S8)}$$

On notable is that the enthalpy of adsorption ($\Delta_{ads}H$) is calculated using the predicted adsorption isotherms obtained by the universal isotherm adsorption model at varying temperatures according to the Clausius-Clapeyron equation shown in Eq. S9.

$$\Delta_{ads}H = -R\frac{\partial(\ln p)}{\partial(1/T)} \quad \text{(Eq. S9)}$$

Then, the formula for calculating COP can be obtained by substitution and simplification.

$$\mathrm{SCE} = \Delta W\left[\Delta_{\mathrm{vap}}H\left(T_{\mathrm{ev}}\right) - C_{\mathrm{p}}^{\mathrm{wf}}\left(T_{\mathrm{con}} - T_{\mathrm{ev}}\right)\right] \quad \text{(Eq. S10)}$$

$$\mathrm{COP_C} = \frac{\Delta W\left[\Delta_{\mathrm{vap}}H\left(T_{\mathrm{ev}}\right) - C_{\mathrm{p}}^{\mathrm{wf}}\left(T_{\mathrm{con}} - T_{\mathrm{ev}}\right)\right]}{C_{\mathrm{p}}^{\mathrm{ad}}\left(T_{\mathrm{des}} - T_{\mathrm{ads}}\right) + C_{\mathrm{p}}^{\mathrm{wf}}\left[W_{\max}\left(T_2 - T_{\mathrm{ads}}\right) + \int_{T_2}^{T_{\mathrm{des}}} W\left(T\right)\mathrm{d}T\right] - \Delta W\Delta_{\mathrm{ads}}H} \quad \text{(Eq. S11)}$$

$$\mathrm{SHE} = \Delta W\left[\Delta_{\mathrm{vap}}H\left(T_{\mathrm{con}}\right) - C_{\mathrm{p}}^{\mathrm{wf}}\left(T_{\mathrm{con}} - T_{\mathrm{ev}}\right) - \Delta_{\mathrm{ads}}H\right] + C_{\mathrm{p}}^{\mathrm{ad}}\left(T_{\mathrm{des}} - T_{\mathrm{ads}}\right) + C_{\mathrm{p}}^{\mathrm{wf}}\left[W_{\min}\left(T_{\mathrm{des}} - T_4\right) + \int_{T_{\mathrm{ads}}}^{T_4} W\left(T\right)\mathrm{d}T\right]$$

(Eq. S12)

$$\mathrm{COP_H} = \frac{\Delta W\left[\Delta_{\mathrm{vap}}H\left(T_{\mathrm{con}}\right) - C_{\mathrm{p}}^{\mathrm{wf}}\left(T_{\mathrm{con}} - T_{\mathrm{ev}}\right) - \Delta_{\mathrm{ads}}H\right] + C_{\mathrm{p}}^{\mathrm{ad}}\left(T_{\mathrm{des}} - T_{\mathrm{ads}}\right) + C_{\mathrm{p}}^{\mathrm{wf}}\left[W_{\min}\left(T_{\mathrm{des}} - T_4\right) + \int_{T_{\mathrm{ads}}}^{T_4} W\left(T\right)\mathrm{d}T\right]}{C_{\mathrm{p}}^{\mathrm{ad}}\left(T_{\mathrm{des}} - T_{\mathrm{ads}}\right) + C_{\mathrm{p}}^{\mathrm{wf}}\left[W_{\max}\left(T_2 - T_{\mathrm{ads}}\right) + \int_{T_2}^{T_{\mathrm{des}}} W\left(T\right)\mathrm{d}T\right] - \Delta W\Delta_{\mathrm{ads}}H}$$

(Eq. S13)

S4. Cooling/Heating performance of working pairs.

Table S6. The number of adsorbents in different range of step position (α).

α	Adsorbent species						Number
	MOFs	Carbon	Zeolites	Silicic materials	Composites	Others	
0.0-0.1	55	3	8	6	–	3	75
0.1-0.2	19	–	–	1	–	–	20
0.2-0.3	15	5	–	–	–	–	20
0.3-0.4	17	2	–	1	–	–	20
0.4-0.5	13	4	–	–	2	–	19
0.5-0.6	6	5	–	–	2	–	13
0.6-0.7	5	7	–	–	1	–	13
0.7-0.8	10	1	1	1	–	–	13
0.8-0.9	8	2	1	2	2	1	16
0.9-1.0	15	7	–	–	–	–	22

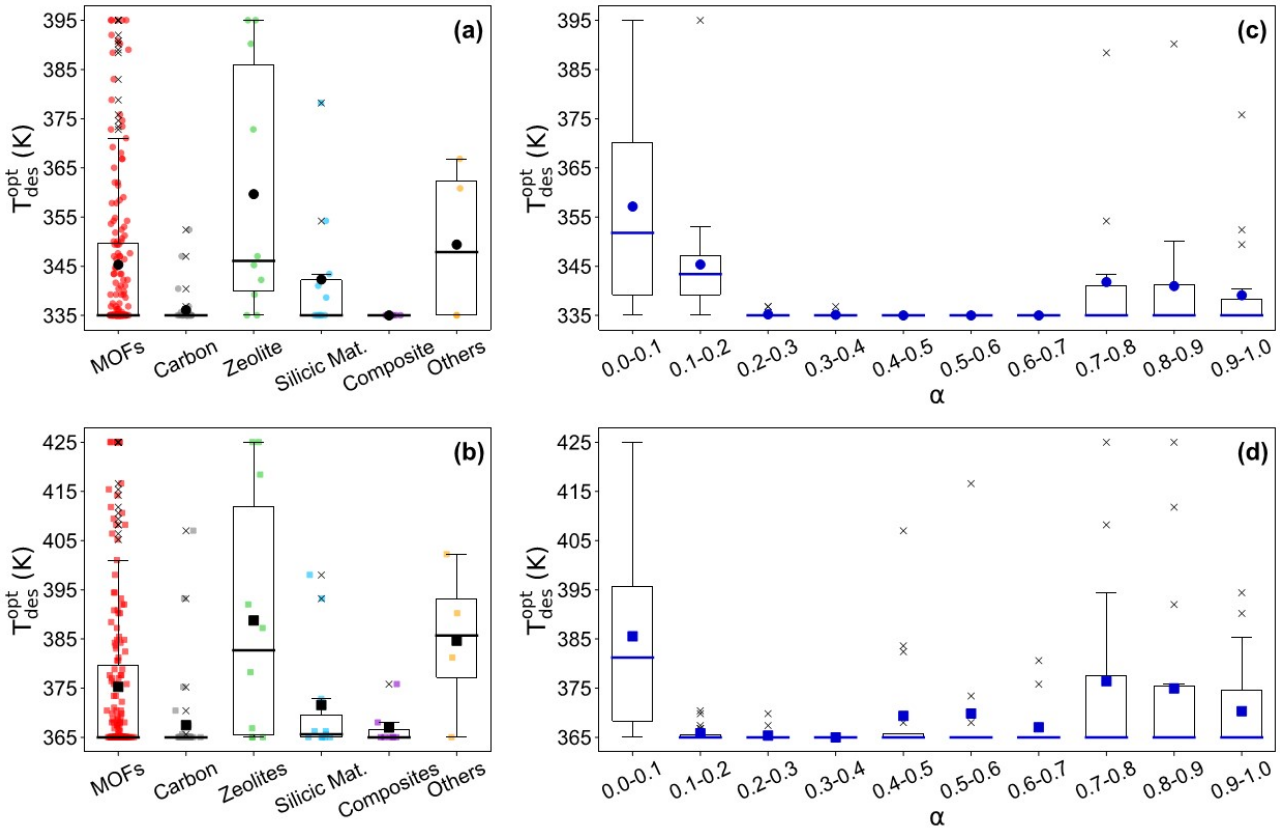

Figure S2. Boxplots of the correlation between optimized desorption temperature (T_{des}^{opt}) and different adsorbent types for (a) cooling and (b) heating. The correlations between T_{des}^{opt} and step position (α) of 231 adsorbents at 298 K for (c) cooling and (d) heating were also displayed.

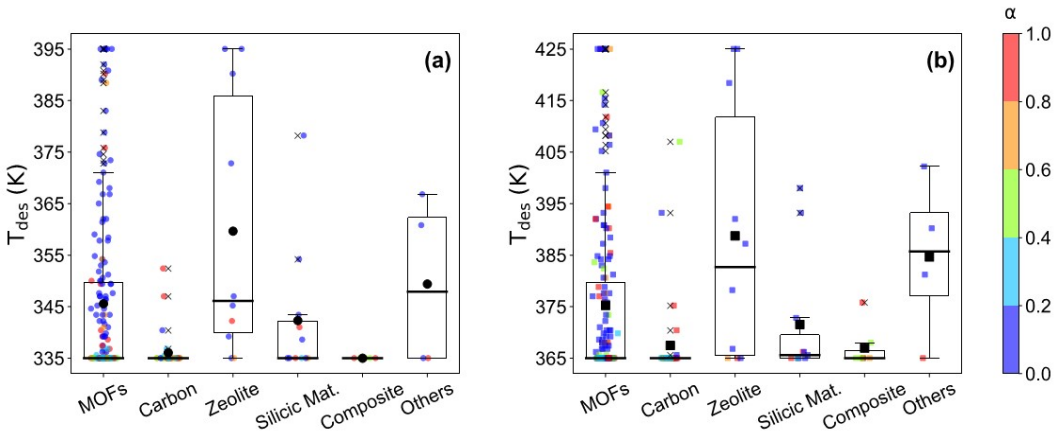

Figure S3. The distribution of different adsorbent species with varying optimized desorption temperature (T_{des}^{opt}), and colors represent the step position (α) of adsorption isotherms for (a) cooling

and (b) heating, respectively.

Because of the positive dependence of COP^{max} on T_{ev}^{opt}, and the complicate correlation between COP^{max} and T_{des}^{opt}, thus we primarily analyzed the correlations between T_{des}^{opt} and the adsorbent types and step positions as shown in Figure S2. Regarding T_{des}^{opt} of different adsorbents, zeolites exhibit the highest T_{des}^{opt} on average for both cooling and heating (Figure S2a and S2b), which can be ascribed to the reported strong interaction between zeolites and water molecules that requires the high temperature for water desorption.[5] In contrast, T_{des}^{opt} of carbon adsorbents is the lowest for cooling and heating due to their weak interaction toward water molecules. The wide distribution of T_{des}^{opt} was observed for MOFs and zeolites, however, 75% of MOFs exhibited the lower T_{des}^{opt} (< 353 K) than zeolites, indicating the high applicability of MOFs for low-temperature heat sources. Although carbon, silicic materials and composites also showed very low T_{des}^{opt}, the low water uptakes greatly restricted their application for adsorption cooling/heating.[6]

On the other hand, the critical role of adsorption isotherm step position (α) in adsorption cooling/heating has been demonstrated in the previous study,[7-8] which is closely correlated with the operational temperatures. Figure S2c and S2d displayed the relationship between T_{des}^{opt} and α of water adsorption isotherm, where the distribution of α between 0 and 1 was observed and the number of different ranges of α was summarized in Table S6. It was revealed that the favorable desorption temperature (T_{des}^{opt}) for adsorbents with $0 < \alpha < 0.1$ was higher compared with the adsorbents with $\alpha > 0.1$, which can be ascribed to the strong hydrophilicity or type-I adsorption isotherm of those adsorbents that requires the high desorption temperature.[5] On the contrary, the lower T_{des}^{opt} is

preferential for the adsorbents displaying a large α especially for those with 0.1 < α < 0.7, which can be ascribed to the easy regeneration of these adsorbents with typical S-shaped or type-V isotherm (relatively large α) according to the previous study.[9] Besides, the relatively high T_{des}^{opt} was inspected for adsorbents with 0.7 < α < 1.0, which was due to the multiple adsorption steps in adsorption isotherms resulting from their hierarchical pores. According to the T_{des}^{opt} distribution of different adsorbents (Figure S3), most adsorbents with α about 0-0.2 are MOFs, implicating the great potential of MOFs at both low and high T_{des}^{opt}.

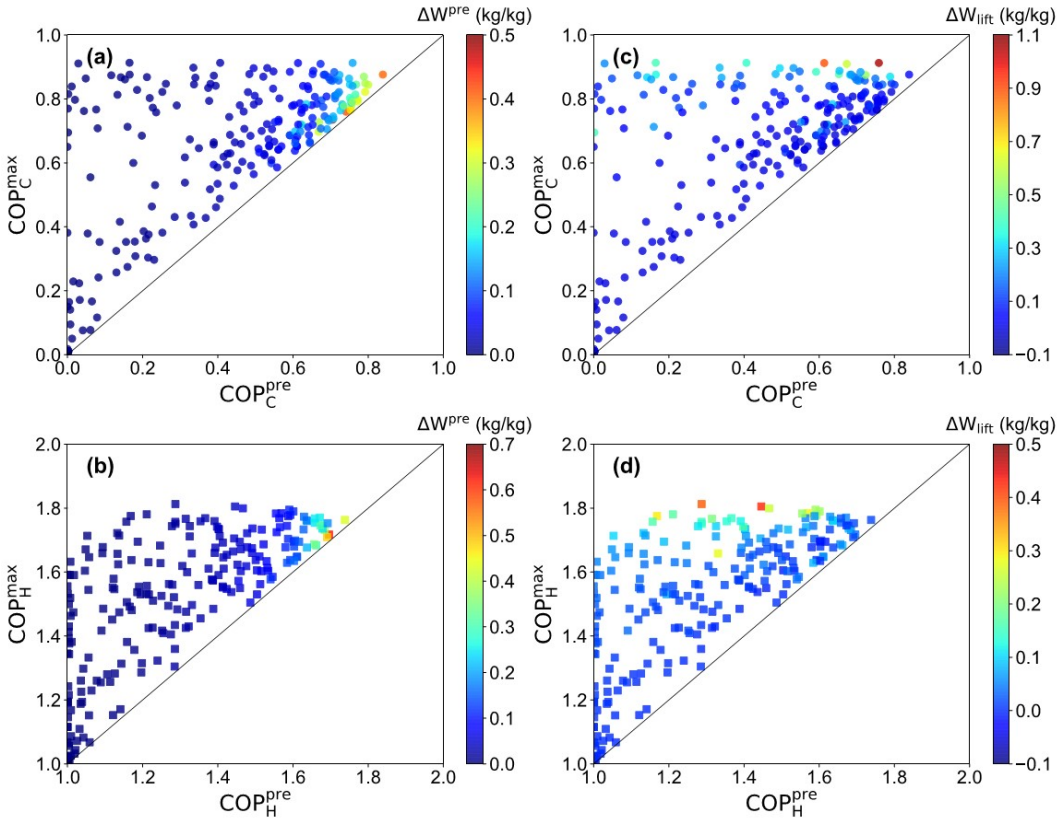

Figure S4. The maximum coefficient of performance (COP^{max}) and COP prior to optimization (COP^{pre}) of 232 adsorbents for (a, c) cooling and (b, d) heating. ΔW^{pre} is water capacity of adsorbents calculated at common conditions in previous work, ΔW_{lift} is the difference between ΔW corresponding COP^{max} and ΔW^{pre}. COP_C was calculated at given $T_{con} = T_{ads} = 303$ K, and COP_H was calculated at

$T_{con} = T_{ads} = 318$ K.

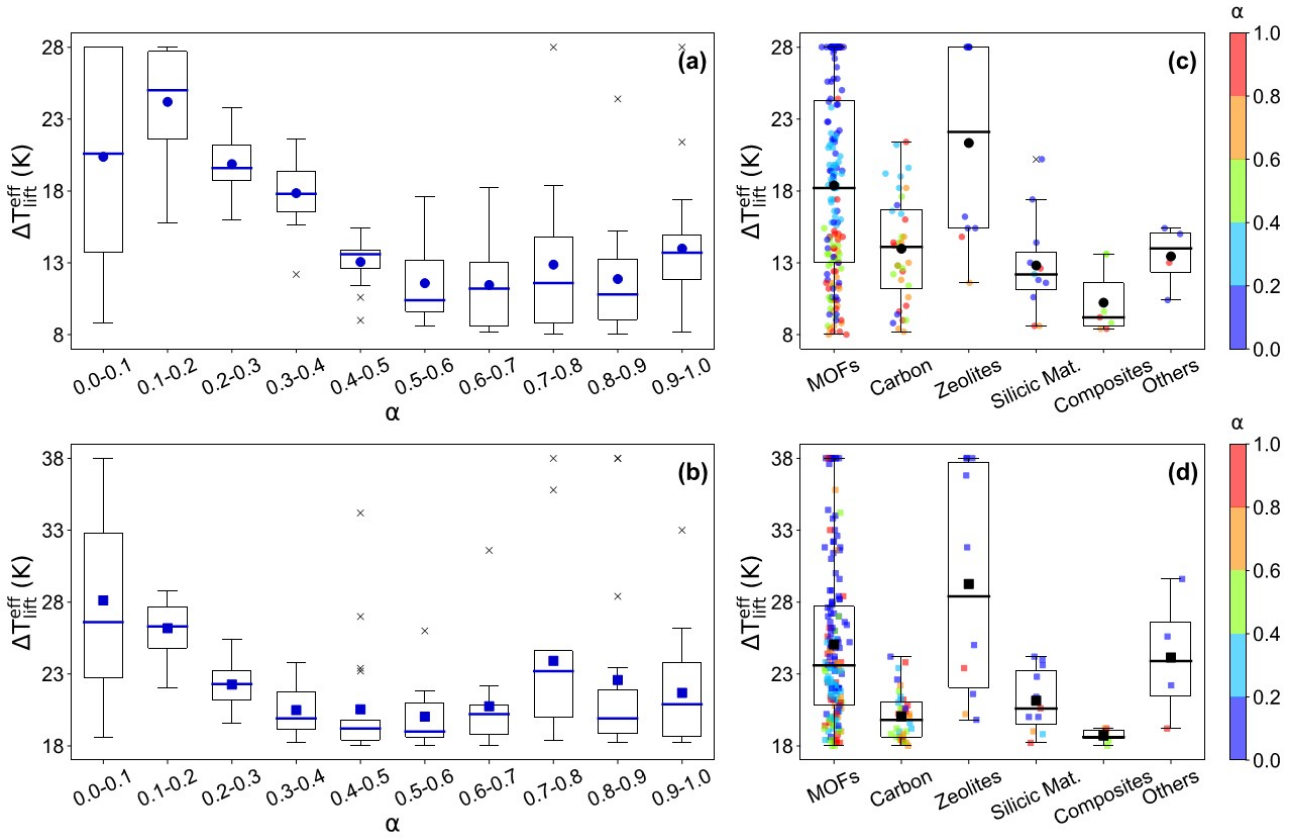

Figure S5. The ΔT^{eff}_{lift} distribution of 231 adsorbents as a function of step position (α) at 298 K for (a) cooling and (b) heating. The ΔT^{eff}_{lift} distribution of different adsorbent types with colored by the step position (α) of adsorption isotherms for (c) cooling and (d) heating, respectively.

References

[1] NIST/ARPA-E Database of Novel and Emerging Adsorbent Materials. https://adsorbents.nist.gov/isodb/index.php#home.

[2] Ng, K. C.; Burhan, M.; Shahzad, M. W.; Ismail, A. B., A Universal Isotherm Model to Capture Adsorption Uptake and Energy Distribution of Porous Heterogeneous Surface. *Sci. Rep.* **2017,** *7* (1), 10634.

[3] Aristov, Y. I.; Tokarev, M. M.; Sharonov, V. E., Universal relation between the boundary temperatures of a basic cycle of sorption heat machines. *Chem. Eng. Sci.* **2008,** *63* (11), 2907-2912.

[4] de Lange, M. F.; Verouden, K. J.; Vlugt, T. J.; Gascon, J.; Kapteijn, F., Adsorption-Driven Heat Pumps: The Potential of Metal-Organic Frameworks. *Chem. Rev.* **2015,** *115* (22), 12205-50.

[5] Henninger, S. K.; Schmidt, F. P.; Henning, H. M., Water adsorption characteristics of novel materials for heat transformation applications. *Appl. Therm. Eng.* **2010,** *30* (13), 1692-1702.

[6] Demir, H.; Mobedi, M.; Ülkü, S., A review on adsorption heat pump: Problems and solutions. *Renewable Sustainable Energy Rev.* **2008,** *12* (9), 2381-2403.

[7] Jeremias, F.; Khutia, A.; Henninger, S. K.; Janiak, C., MIL-100(Al, Fe) as water adsorbents for heat transformation purposes—a promising application. *J. Mater. Chem.* **2012,** *22* (20), 10148-10151.

[8] Aristov, Y. I., Challenging offers of material science for adsorption heat transformation: A review. *Appl. Therm. Eng.* **2013,** *50* (2), 1610-1618.

[9] Lenzen, D.; Zhao, J.; Ernst, S. J.; Wahiduzzaman, M.; Ken Inge, A.; Frohlich, D.; Xu, H.; Bart, H. J.; Janiak, C.; Henninger, S.; Maurin, G.; Zou, X.; Stock, N., A metal-organic framework for efficient water-based ultra-low-temperature-driven cooling. *Nat. Commun.* **2019,** *10* (1), 3025.